



ISSN: 0975-833X

RESEARCH ARTICLE

DIFFERENT PROPERTY STUDIES ON ALUMINIUM SUBSTITUTED ZnO NANOCRYSTALS
SYNTHESIZED BY SOL-GEL AUTO COMBUSTION TECHNIQUE

¹Gaikwad, H. K., ²Bodke, M. R. and ^{1,*}Lokhande, P. D.

¹Department of Chemistry, Savitribai Phule Pune University, Pune, Maharashtra, India

²Department of Electronic Science, Modern College of Arts, Science and Commerce Shivajinagar, Pune, Maharashtra, India

ARTICLE INFO

Article History:

Received 21st December, 2014
Received in revised form
04th January, 2015
Accepted 04th February, 2015
Published online 31st March, 2015

Key words:

Sol-gel auto combustion route, XRD,
Hexagonal, Uv-Visible spectroscopy,
Red shift.

Copyright © 2015 Gaikwad et al. This is an open access article distributed under the Creative Commons Attribution License, which permits unrestricted use, distribution, and reproduction in any medium, provided the original work is properly cited.

ABSTRACT

Undoped and 20at. % Al doped ZnO nanocrystals were successfully prepared by Sol-gel auto combustion route. Structural properties were studied from XRD pattern. The hexagonal wurtzite structure was detected. The crystallite size was calculated using Sherrer's formula. Crystallite size determined 5.68nm and 4.05nm for undoped and 20at.% Al concentration. Optical study was completed by UV-Visible spectroscopy. Absorption peaks estimated at 352 nm and 366 nm. Energy band gap were calculated from Tauc's plots. 3 eV and 3.05 eV are the values of Eg for ZnO and 20 at.% Al doped ZnO nanocrystals. It confirms that red shift in the energy band gap.

INTRODUCTION

Zinc is one of the diluted magnetic direct band gap semiconductor with the energy band gap (3.37 eV) and binding energy (60 meV). ZnO belongs to n-type semiconductors. ZnO is used for optical sensors and light emitters as optoelectronic applications (R.F. Service, Science 1997 and Makino *et al.*, 2000), Including this it is also used as surface acoustic wave (SAW) devices, gas sensing devices, piezoelectric devices and solar cells (Fortunato *et al.*, 2005) (Gong *et al.*, 2006) (Song *et al.*, 2006) (Jeong *et al.*, 2003) (Zhang *et al.*, 2006) and (Verma *et al.*, 2010). Undoped and Al doped ZnO nanocrystals were prepared by various methods, such as sol-gel (Serier *et al.*, 2009), spray pyrolysis (Ogi *et al.*, 2009), chemical precipitation (Du *et al.*, 2006), and hydrothermal processes (Zhang *et al.*, 2005). The sol-gel process had attracted considerable attention because it is simplest, cost effective and the crystalline quality of Al-doped nanocrystals (Serier *et al.*, 2009 and Tsubota *et al.*, 1997). Lotus and Cheng *et al.*, investigated the band gap and conductivity of Al-doped ZnO nanofibers and ceramics with the concentrations 1at. % to 4at. % (Lotus *et al.*, 2010) and (Cheng *et al.*, 2009) Sonja Hartner *et al.* (2009) reported that the higher percentage of Al doping is possible under high temperature nonequilibrium conditions compared to wet chemical synthesis.

They have synthesized Al doped ZnO nanocrystals by chemical vapour synthesis for 5.39%, 7.03%, 7.74%, 16.79% and 37.63% of Al concentrations. We were no literature available on 20at. % aluminium doped ZnO nanocrystal. Therefore we have decided to synthesize and study the different properties of 20at. % Al doped ZnO nanocrystals. We have synthesized 20at.% Al doped ZnO nanocrystals by sol-gel auto combustion route using the stirring materials zinc nitrate, aluminium nitrate and N N-Dimethyl formamide as fuel for combustion.

Experimental

Starting materials used for synthesis of undoped and Al doped ZnO nanocrystals were zinc nitrate, aluminium nitrate and N-N Dimethyl formamide N-NDMF. All chemicals were of analytical grade, used without further purification. The mixture zinc nitrate and N-NDMF with their appropriate weights was stirred continuously for 2h at 70^oC temperature to get completely dissolved solution. Then the clear solution was kept on hot plate at 170^oC for 3h for formation of jel. Further heating auto combustion of jel takes place and the undoped ZnO nanomaterials are formed. For the synthesis of Al doped ZnO nanocrystals, zinc nitrate and aluminium nitrate with their appropriate weights mixed with 20 ml each of N-NDMF in the separate beakers and stirred vigorously for 3h at 70^oC. Then the prepared clear solutions were added together and mixed thoroughly by stirring again for 1h, and then kept on hot plate

*Corresponding author: Lokhande,

Department of Chemistry, Savitribai Phule Pune University, Pune, Maharashtra, India.

at 170°C for 3h for formation of gel. Further heating of gel combustion takes place and the undoped ZnO and Al doped ZnO nanocrystals were formed. The material was annealed at 600°C. For getting uniform crystallite size the samples were grind for 15min.

RESULTS AND DISCUSSION

Structural study

Structural study has been completed by X-ray diffraction technique. XRD pattern for ZnO and 20at% Al doped ZnO were as shown in Fig. 1 (a) and (b). From The diffraction peaks estimated in pure ZnO were (100), (002), (101), (102), (110) and (103). There were ten diffraction peaks were estimated for 20 at. % Al doped ZnO nanocrystals as (100), (002), (101), (102), (110), (200), (112), (201) and (103). The diffraction peaks (200), (112) and (201) were disappeared in undoped ZnO, it may be due to the sample annealed at 600°C. Kumar *et al.* (2011) reported that, there was slight shifting in (002) peak position to the higher angles with the substitution of Al into ZnO lattice, it may be due to smaller radii of Al³⁺, 2011. In our research work the diffraction peaks for 20at.% Al doped ZnO nanocrystals are broaden and shifted to lower values of 2θ than undoped ZnO nanocrystals. XRD diffraction data compared with JCPDS card and it was well matched with JCPDS card no. (75-1526), it confirms the nanocrystals are having hexagonal (wurtzite) structure. The crystallite size of the ZnO nanocrystals was estimated using Scherrer's formula and it decreased from 5.68 nm to 4.05 nm with 20 at. % Al doping concentration into ZnO. Crystallite size of Al doped ZnO nanocrystals was smaller than Undoped ZnO nanocrystals. It might be due to quantum confinement effect caused by the substitution of Al³⁺ into ZnO lattice. The lattice parameters were calculated from the XRD data and recorded in table 1. The lattice constants values 'a' and 'c' were very closer to the standard values recorded in JCPDS card values 3.22 nm and 5.2nm respectively. Crystallite size, X-ray density and APF values were decrease with 20at. % Al cocentration into ZnO lattice.

Chemical groups and bonding study

Chemical groups and chemical bonding study has been completed by fourier transform infrared spectroscopy. FTIR (JASCO FTIR-4100, JAPAN) spectra's were recorded at room temperature. Figure 4 (a) and (b) shows the FTIR spectra for undoped and 20at. % Al doped ZnO nanocrystals annealed at 600°C. The broad band formed around 3453 cm⁻¹ in 20at.% Al doped ZnO nanocrystals was typically due to stretching and bonding modes of hydroxyl (O-H) group of H₂O (Nakamoto *et al.*, 1991). But this broad band divided into two bands around 3597 cm⁻¹ and 3708 cm⁻¹, which was shifted to the higher wave number. The additional weak band and shoulders at 2929 cm⁻¹ and 1526 cm⁻¹ for undoped ZnO and around 2339 cm⁻¹ and 1502 cm⁻¹ for 20at. % Al doped ZnO nanocrystals annealed at 600°C temperature, it may be due to nano structural formation or quantum confinement effect of the samples. The absorption bands observed around 1328 cm⁻¹ and 1374 cm⁻¹ for undoped and Al doped ZnO nanocrystals were due to CO₂ stretching. The peaks observed around 807 cm⁻¹ for 20at.% Al doped ZnO nanocrystals is due to Zn-Al-O stretching and 873 cm⁻¹ for undoped ZnO nanocrystals was due to Zn-O stretching. In FTIR spectra for undoped ZnO nanocrystals, the IR peak observed around 650 cm⁻¹ and 620 cm⁻¹ for 20at. % Al doped ZnO nanocrystals were due to asymmetric bending. Vibration bands and stretching bands in the range 500–900cm⁻¹, associated with the vibrations of metal– oxygen (Deng *et al.*, 2002), aluminum–oxygen (Nakamoto *et al.*, 1991) and metal– oxygen– aluminum (De Suza *et al.*, 2009). The Five IR peaks were observed for 20at.% Al doped ZnO nanocrystals ZnO in region 421 cm⁻¹ to 498 cm⁻¹ were due to Zn-O vibrational modes, where as six peaks were observed in the region around 419 cm⁻¹ to 493 cm⁻¹ for undoped ZnO nanocrystals.

Optical Study

UV-Visible Spectroscope was used to complete the optical study of undoped and 20at% Al doped ZnO nanocrystal samples.

Table 1. Lattice constants and lattice parameters of ZnO nanocrystals undoped and 20 at.% Al doped ZnO nanocrystals.

Samples	Lattice Constants			Crystallite Size (nm)	X-ray density (gm/cm ³)	Volume of unit cell (Å ³)	% APF
	a (nm)	c (nm)	a/c ratio				
Undoped ZnO	3.1996	5.1129	0.6257	5.6807	5.9643	45.3304	75.63
20 at. % Al doped ZnO nanocrystals	3.2100	5.1666	0.6214	4.0530	5.8640	46.1052	75.09

Morphological Study

Figure 2 shows the SEM images with 30 μm magnification of undoped and 20at. % Al doped ZnO nanocrystals. Undoped ZnO particles were transparent and pure crystalline But the agglomeration of the particles was clearly observed in Al doped ZnO nanocrystals. It might be due to the decrease in grain size around 4 nm, than undoped ZnO sample. Chen *et al.* (2008) reported that the crystallinity of the ZnO nanocrystals decreases with large amount of Al doping into ZnO resulted in lattice disorder. In our study it is clearly observed from the SEM images for undoped and 20at. % Al doped ZnO samples.

Figure 4 (a) and (b) shows the absorption spectra for undoped and Al doped ZnO nanocrystals annealed at 600°C respectively. The absorption spectra of undoped and Al doped ZnO nanoparticle samples shows a single absorption peak. It confirms that there were no impurities found in prepared samples. The absorption peaks reported at 352 nm and 466 nm for undoped and 20at% Al doped ZnO nanocrystals. The blue shift in the absorption peaks detected from undoped to Al doped ZnO nanocrystals. A. Alkahlout *et al.* reported that the blue shift of the absorption edge in the zinc oxide nanocrystals can be assigned to the direct transition of electrons (Alkahlout *et al.*, 2014).

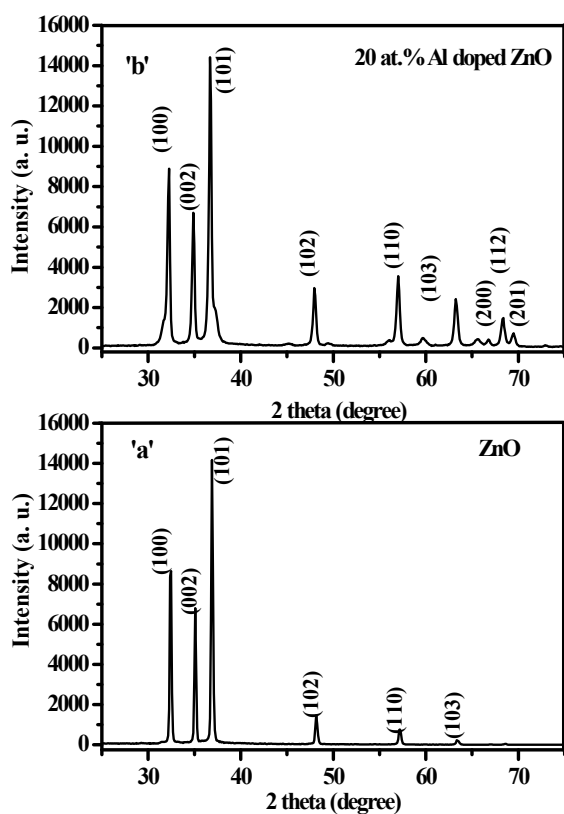


Fig. 1 (a) and (b) XRD pattern for ZnO and Al doped ZnO nanocrystals

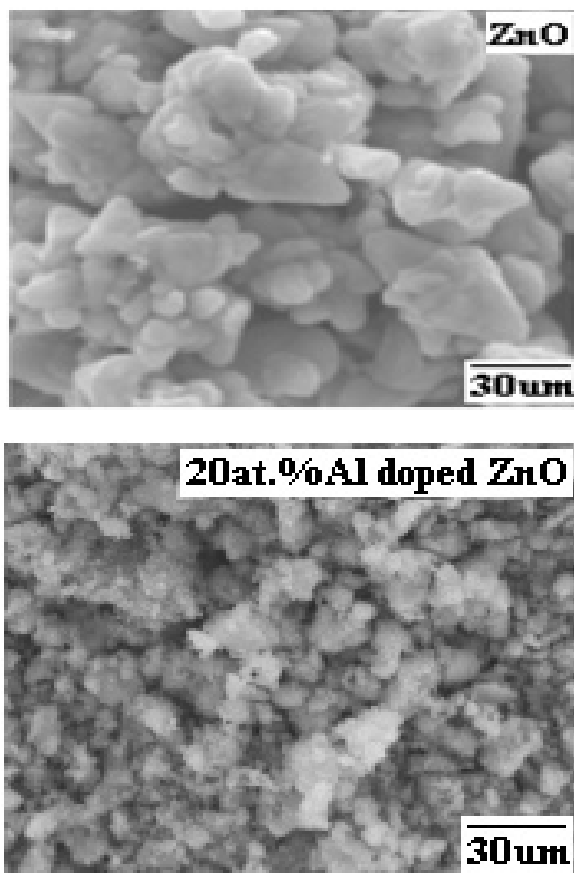


Fig. 2. SEM images for undoped and Al doped ZnO nanocrystals

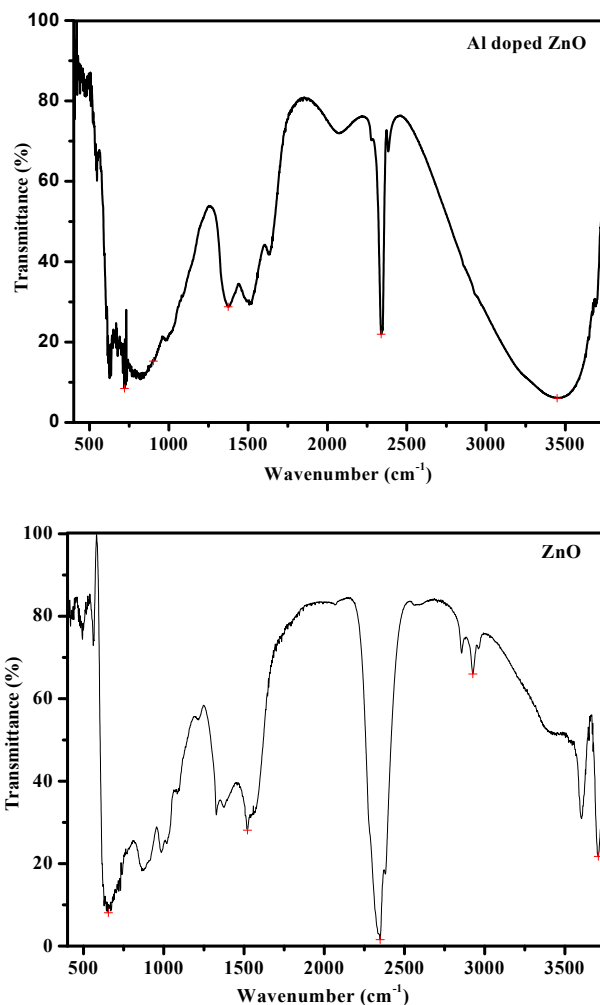


Fig.3. FTIR spectra for undoped and Al doped ZnO nanocrystals

Optical energy band gaps for undoped and Al doped ZnO nanoparticle samples were determined from Tauc's plots as shown in Figure 5 (a) and (b). Y. Zhang *et al.* (2011) reported that the Al doped ZnO nanopowder revealed red shift at 6at.% Al concentration. The energy band gap values recorded for undoped and 20at% Al doped ZnO nanoparticle with their crystallite sizes 5.68 nm and 4.05 nm are 3 eV and 3.05 eV respectively. It evidenced that energy band gap value increased for 20at% Al doping into ZnO. It revealed the red shift in energy band gap. The quantum confinement effect theory explains that the value of energy band gap of semiconductor will increase with the decrease in crystallite size (Wang *et al.*, 2004) and (Shrinivasan *et al.*, 2007).

Conclusion

Undoped and 20at. % Al doped ZnO quantum dots were prepared by Sol-gel auto combustion route. There were no secondary phases observed in XRD pattern. Slight shifting of diffraction peaks to lower 2θ values, it might be due to smaller radii of Al³⁺ substituted into ZnO lattice. Morphological study has been completed using SEM. FTIR were completed to study chemical bonding and stretching. The purity of the prepared sample is confirmed from single absorption peak in absorption spectra and the energy band gap values 3 nm and 3.05 nm from UV-Visible study. The energy band gap E_g increased when

ZnO was doped with Al. It evidenced that red shift in the energy band gap.

REFERENCES

- Alkahlou, t A., Al Dahoudi, N., Grobelsek, I., Jilav, i M. and De, P.W. 2014. Oliveira Hindawi Publishing Corporation *Journal of Materials*, p://dx.doi.org/10.1155/2014/235638
- Chen K.J., Fang T.H., Hung F.Y., Ji L.W., Chang S.J., Young S.J., Hsiao Y.J. (2008) *Applied Surface Science*, 254,5791–5795
- Cheng, H, Xu X. J., Hng, H., H. and Ma J. 2009. *Ceram Int* 35:3067. doi: 10.1016/j.ceramint.2009.04.010
- Deng, Z.,X., Wang, C., Sun, X.,M. and Li, Y., D. 2002. *Inorg. Chem.* 41, 869–873. doi: 10.1063/1.1577819.
- Du, S., F, Tian, Y., J, Liu, H., D, Liu, J. and Chen, Y.,F. 2006. *J Am Ceram Soc* 89:2440. doi:10.1111/j.1551-2916.2006.01093.x
- Fortunato, E., Barquinha, P., A. Pimentel, A., Goncalves, A., Marques, A., Pereira, L. and Martins, R., 2005. *Thin Solid Films* 487, 205–211.
- Gong, H., Hu, J., Q., Wang, J.,H., Ong, C.,H. and Zhu F.R. 2006. *Sens. Actuators B* 115, 247–251.
- Jeong, I., S., Kim, J.,H. and Im, S. 2003. *Appl. Phys. Lett.* 83, 2946–2948.
- Kumar R. S., Sathyamoorthy R., Saudhagar P., Matheswaran P., Hrudhya C. P., Kang Y. S. 2011. *Physica., E* 43, 1166-1170.
- L.K.C. de Souza, J.R. Zamian, G.N. da Rocha Filho, L.E.B. Soledade, I.M.G. dos Santos, A.G. Souza, T. and Scheller, R.S. 2009. *Angelica, Dyes Pigments* 81 pp187–192.
- Lotus, A.F., Kang Y.C., Walker, J.I., Ramsier R. D. and Chase, G. G. 2010. *Mater Sci Eng B* 166:61. doi:10.1016/j.mseb.2009.10.001
- Makino, T., Chia, C.,H., Nguen, T.,T. and Segawa, Y. 2000. *Appl. Phys. Lett.* 77, 1632–1634.
- Nakamoto, K., in; 1991. *Infrared Spectra of Inorganic and Coordination Compounds*, Wiley, 1997 New York.
- Nakamoto, K., in; 1991. *Infrared Spectra of Inorganic and Coordination Compound*, 4th ed., Chemical Industry Press, Beijing.
- Ogi, T., Hidayat, D., Iskandar, F., Purwanto, A. and Okuyama, K (2009) *Adv Powder Technol* 20:203. doi:10.1016/j.appt.2008.09.002
- R.F. Service, *Science* 895. 1997. 276.
- Serier, H., Gaudon, M. and Me'ne'trier, M. 2009. *Solid State Sci* 11:1192. doi:10.1016/j.solidstatesciences.2009.03.007
- Shrinivasan, G., Rajendra kumar R. T., and Kumar . 2007. *J. Opt. Matter* 30:314. Doi: 10.1016/j.optmat.2006.11.075
- Song, J., Zhou J. and Wang, Z., L. 2006. *Nano Lett.* 6, 1656–1662.
- Sonja, H., Moazzam, A., Christof, S., Markus, W. and Hartmut W. 2009. *Nanotechnology* 20, 445701 (8pp) doi:10.1088/0957-4484/20/44/445701.
- Tsubota, T., Ohtaki, M., Eguchi, K. and Arai, H. 1997. *J Mater Chem.*, 7:85
- Verma, A., Khan, F., Kar, D., Chakravarty, B.C., Singh S.N. and Husain M. 2010. *Thin Solid Films* 518:2649. doi:10.1016/j.tsf.2009.08.010
- Wang, Y. G., Lau S. P., Lee H. W., Yu S. F., Tay B. K., Zhang X. H., Hng H. H. 2004. *J. Appl Phys* 94:354.
- Zhang, H., Yang, D., Li, S.,Z., Ma, X.,Y., Ji YJ, Xu, J. and Que, D.,L. 2005. *Mater Lett* 59:1696. doi:10.1016/j.matlet.2005.01.056
- Zhang, Y., Yang Y., Zhao J., Tan R., Wang W., Cui P. and Song W. 2011. *J. Mater Sci* 46:774-780.
- Zhang, Z., Lu, Y., M., Shen, D., Z., Yao, B., Zhang, J.Y., Li, B.H., Zhao, D.,X., Fan X.W. and Tang Z.K. 2006. *Appl. Phys. Lett.* 88,031911.
